Secretion of Tat-dependent halolysin SptA capable of autocatalytic activation and its relation to haloarchaeal growth

Xin Du,[1] Moran Li,[1] Wei Tang,[1] Yaoxin Zhang,[1] Li Zhang,[1] Jian Wang,[1] Tingting Li,[1] Bing Tang[1,2] and Xiao-Feng Tang[1,2]*
[1]*State Key Laboratory of Virology, College of Life Sciences*, Wuhan University, Wuhan, China.
[2]*Hubei Provincial Cooperative Innovation Center of Industrial Fermentation*, Wuhan, China.

Summary

Halolysins are Tat-dependent extracellular subtilases of haloarchaea. Whether halolysins can be activated before transport across the cytoplasmic membrane in a folded state and how haloarchaea minimize the risk of intracellular activation of halolysins and proteolysis of cellular proteins are unknown. Here, we report that both the precursor and proform of halolysin SptA from *Natrinema* sp. J7-2 mature autocatalytically, and the SptA maturation proceeds less efficiently in the presence of KCl than NaCl. When produced in *Haloferax volcanii*, most SptA molecules are secreted into the culture medium, but a small number of molecules can be activated intracellularly, affecting the cell's growth. Furthermore, retardation of SptA secretion in *Hfx. volcanii* via mutation of the Tat signal peptide leads to intracellular accumulation of the active enzyme and subsequent cell death. Although the Sec signal peptide can mediate SptA secretion in *Hfx. volcanii*, the secreted protein undergoes proteolysis. In *Natrinema* sp. J7-2, SptA is secreted primarily during stationary phase, and the intracellular accumulation of mature enzyme occurs during the stationary and death phases. The growth phase-dependent synthesis of SptA, highly efficient secretion system, and high intracellular KCl concentration, contribute to the suppression of premature activation of this enzyme in *Natrinema* sp. J7-2.

Introduction

The three domains of life use a variety of pathways to translocate different proteins across the cytoplasmic membrane. The general secretory (Sec) pathway is the only known universally conserved protein translocation pathway and is used to move most secreted proteins across the cytoplasmic membrane in an unfolded state, either co- or post-translationally (Pohlschröder *et al.*, 1997). The twin-arginine translocation (Tat) pathway is present in many bacteria and archaea, but in eukaryotes it is found only in chloroplasts. The Tat pathway translocates folded proteins across the cytoplasmic or thylakoid membranes (Pohlschröder *et al.*, 1997; Berks *et al.*, 2005). In contrast to other organisms that route most of their secretory proteins to the Sec pathway, haloarchaea and *Streptomyces* species export the majority of their secretory proteins via the Tat pathway (Bolhuis, 2002; Rose *et al.*, 2002; Widdick *et al.*, 2006). In addition, genetic analyses have shown that the haloarchaeal Tat pathway is essential for viability (Dilks *et al.*, 2005; Thomas and Bolhuis, 2006). Haloarchaea thrive in hypersaline (2–5.2 M NaCl) environments such as solar salterns, salt lakes, and salt deposits (Grant, 2004) and accumulate molar concentrations of intracellular KCl to osmotically balance high external NaCl concentrations (Pérez-Fillol and Rodríguez-Valera, 1986; Martin *et al.*, 1999). It has been hypothesized that in response to hypersaline conditions, haloarchaea route secretory proteins to the Tat pathway so they can be correctly folded in a controlled cytoplasmic environment where chaperones are present (Pohlschröder *et al.*, 2004). Alternatively, under high internal salt concentrations, haloarchaeal proteins may fold rapidly to prevent aggregation before translocation, and thus are routed to the Tat pathway (Bolhuis, 2002; Rose *et al.*, 2002).

Many haloarchaea secrete proteases that degrade proteins and peptides in the natural environment (De Castro *et al.*, 2006). Almost all of the extracellular proteases isolated from haloarchaea are serine proteases, and most of them appear to belong to the subtilisin-like serine protease (subtilase) superfamily (Siezen and Leunissen, 1997) known as halolysins (Kamekura *et al.*, 1992; De Castro

et al., 2006). Extracellular subtiliases are generally produced as inactive precursors composed of a signal peptide, an N-terminal propeptide, and a mature domain. The signal peptide mediates the translocation of the enzyme across the cytoplasmic membrane, where it is cleaved by a signal peptidase. The N-terminal propeptide usually functions as an intramolecular chaperone to assist in the folding of the mature domain and also as a potential inhibitor of its cognate mature enzyme (Shinde and Thomas, 2011). The maturation of subtilases has been extensively studied for bacterial subtilisins E and BPN′, of which the N-terminal propeptide is processed in an autocatalytic manner, mediated by the active site of the mature domain (Gallagher *et al.*, 1995; Yabuta *et al.*, 2001). Characterized halolysins include 172P1 from *Natrialba asiatica* (Kamekura *et al.*, 1992), R4 from *Haloferax mediterranei* (Kamekura *et al.*, 1996), SptA and SptC from *Natrinema* sp. J7 (Shi *et al.*, 2006; Zhang *et al.*, 2014), and Nep from *Nab. magadii* (De Castro *et al.*, 2008). Each of these halolysins is synthesized as a precursor containing a Tat signal peptide, an N-terminal propeptide, a subtilisin-like catalytic domain, and a C-terminal extension (CTE). Mutation analyses of the Tat signal peptides of SptA and Nep have shown that these halolysins are Tat-dependent substrates (Shi *et al.*, 2006; Ruiz *et al.*, 2012). Nep and SptC reportedly mature autocatalytically (Ruiz *et al.*, 2012; Zhang *et al.*, 2014). These findings raise interesting questions about whether Tat-dependent halolysins can be prematurely activated before translocation across the cytoplasmic membrane in a folded state and how haloarchaea minimize the risk of premature activation of halolysins and associated proteolytic damage to cellular proteins. To the best of our knowledge, these issues have yet to be addressed.

The haloarchaeon *Natrinema* sp. J7 was originally isolated in the early 1990s from a salt mine in Hubei Province, China (Shen and Chen, 1994) and grows optimally at ~ 3.1–3.8 M NaCl. We previously cloned three halolysin-encoding genes from the strain J7 genome, designated *sptA*, *sptB* (these two genes are arranged in tandem; AY800382), and *sptC* (DQ137266). SptA and SptC have been characterized in terms of enzymatic properties and functions of their CTEs (Shi *et al.*, 2006; Xu *et al.*, 2011; Zhang *et al.*, 2014). SptA is stable at high salt concentrations and exhibits higher enzymatic activity in NaCl solution than KCl solution (Shi *et al.*, 2006). The mature form of SptA is composed of the subtilisin-like catalytic domain and the CTE domain that not only confers extra stability to the enzyme but also assists in enzymatic activity on protein substrates by facilitating binding at high salinities (Xu *et al.*, 2011). SptA contains six Cys residues, of which the residues Cys^{303} and Cys^{338} within the CTE domain form a disulfide bond that makes this domain resistant to autocleavage and proteolysis under hypotonic conditions (Xu

et al., 2011). The complete genome of *Natrinema* sp. J7-2 (a subculture of strain J7 that lacks the plasmid pHH205) has been sequenced (Feng *et al.*, 2012). Our recent proteomic analysis of the secretome of strain J7-2 identified more Tat substrates than Sec substrates (Feng *et al.*, 2014), supporting previous *in silico* predictions that the Tat pathway is more extensively used for secretion of haloarchaeal proteins. In that study, we detected SptA in the late-log/early-stationary-phase J7-2 culture supernatant rather than the mid-log-phase culture supernatant, prompting us to elucidate the mechanism of SptA activation and determine the relationship between SptA secretion and activation and haloarchaeal growth.

In the present study, *in vitro* analyses revealed that both the precursor and proform of SptA mature via stepwise autoprocessing of the N-terminal propeptide. Although most SptA molecules were secreted into the culture medium in the active mature form when produced by *Haloferax volcanii*, a small number of SptA molecules were activated intracellularly, affecting the growth of this haloarchaeon. Furthermore, retardation of SptA secretion by *Hfx. volcanii* via mutation of its Tat signal peptide led to intracellular accumulation of active mature enzyme, resulting in death of the host cells. In contrast, SptA was produced and secreted by strain J7-2 primarily during the stationary phase, and intracellular accumulation of the active mature form occurred during the stationary and death phases. This represents the first experimental data demonstrating intracellular activation of a Tat-dependent halolysin and provides evidence suggesting that SptA activation affects haloarchaeal growth.

Results

Both the precursor and proform of SptA are autocatalytically processed into the active mature form *in vitro*

To investigate the SptA maturation process *in vitro*, recombinant SptA precursor (SptAH) and its derivatives (Fig. 1A) were produced in *Escherichia coli* and purified under denaturing conditions (8 M urea) using His-tag affinity chromatography. The apparent molecular weights of the recombinant proteins as determined by SDS-PAGE analysis were higher than their predicted molecular weights (Fig. 1B), which is a common feature of halophilic proteins with a high content of acidic residues (Madern *et al.*, 2000). A few minor protein bands were present in some purified samples (Fig. 1B) and could be detected by anti–His-tag immunoblot analysis (data not shown), indicating that they were degradation products of the target proteins.

A sample of denatured SptAH was diluted 10-fold in buffer A containing 4 M NaCl and then incubated at 37°C to allow enzyme refolding and processing. During the early
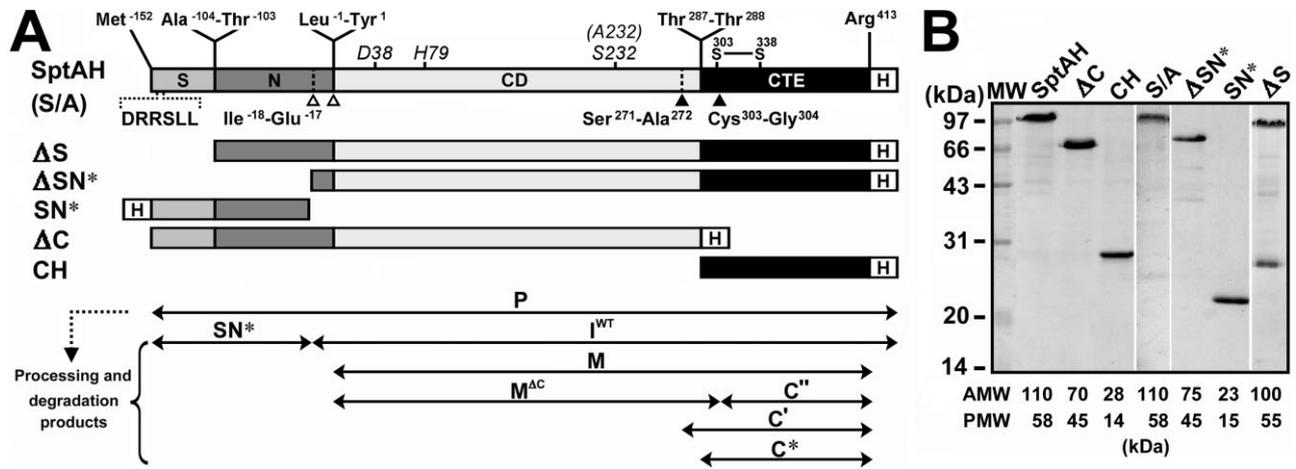
Fig. 1. Schematic representation of the primary structures (A) and SDS-PAGE analysis (B) of purified SptAH and its derivatives.
A. The signal peptide (S), the N-terminal propeptide (N), the catalytic domain (CD), the C-terminal extension (CTE), and the fused His-tag (H) are indicated. The locations of the Tat motif (DRRSLL) in the signal peptide, the active-site residues, the Cys^{303}-Cys^{338} disulfide bond, and the N- and C-terminal residues of each region are shown. Open and closed arrowheads indicate the identified autoprocessing and degradation sites respectively. Double-headed arrows represent the precursor (P) and its processing and degradation products identified during maturation of SptAH (indicated by arrowheads in Fig. 2A).
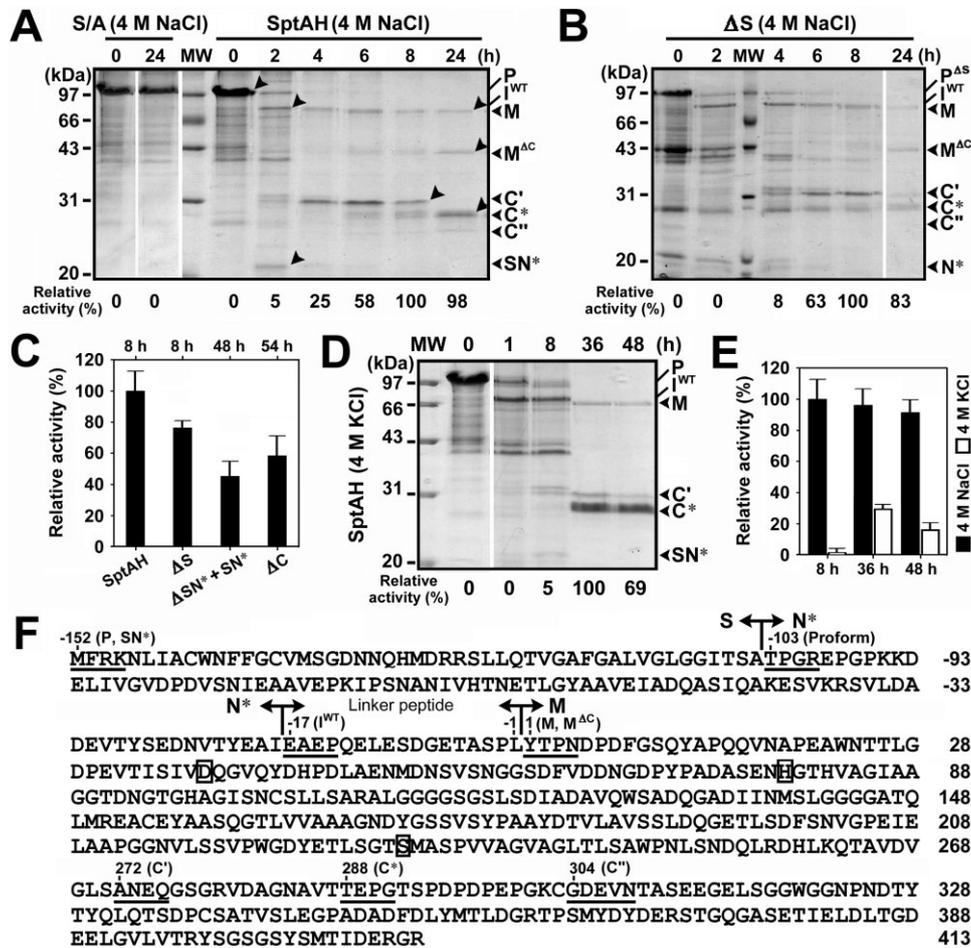B. Purified samples of SptAH and its derivatives were subjected to SDS-PAGE analysis. The predicted molecular weight (PMW) of each protein was calculated based on the amino acid sequence. Apparent molecular weight (AMW) was determined by SDS-PAGE analysis.

stage of incubation, SptAH was cleaved into two major products, designated I^{WT} and SN* (0–2 h, Fig. 2A). N-terminal sequencing of the two products revealed that the cleavage occurred at Ile^{-17}-Glu^{-18} (Fig. 1A and Fig. 2F). As incubation time increased, I^{WT} was further processed into product 'M', accompanied by the degradation of SN* and the complete release of proteolytic activity (4–8 h, Fig. 2A). The sequence of the first four amino acids of M was determined to be YTPN (Fig. 2F), identical to that of mature SptA produced by *Natrinema* sp. J7 (Shi *et al.*, 2006). This result demonstrates that the 17 N-terminal residues of the intermediate (I^{WT}) are truncated to generate the mature form (M, Fig. 1A). Therefore, the N-terminal propeptide of SptA consists of a core domain (N*) and a 17-residue linker peptide. An active-site variant of SptAH (S/A) was constructed by replacing the catalytic residue Ser^{232} with Ala (Fig. 1A). In contrast to SptAH, the active-site variant S/A remained unprocessed under the same conditions (Fig. 2A), suggesting that the active site mediates the processing of the N-terminal propeptide and that the maturation of SptA proceeds autocatalytically. We observed that the rate of SptAH maturation slowed at lower protein concentrations and could be accelerated by the addition of proteinase K (Fig. S1). This result suggests that active enzyme that matures earlier during the maturation process most likely triggers an exponential cascade by catalyzing the degradation of SN* and the intermolecular truncation of the linker peptide, as described for other subtilases (Zhu *et al.*, 2013).

Some degradation products were also detected during the maturation of SptAH. The N-terminal sequence of

product $M^{\Delta C}$ was identical to that of M (YTPN, Fig. 2F), and the accumulation of $M^{\Delta C}$ and C″ correspond to two previously identified products (SptAΔC110 and SptAC110) derived from mature SptA under reducing conditions in which the mature form undergoes autocleavage at Cys^{303}-Gly^{304} due to reduction of the Cys^{303}-Cys^{338} disulfide bond that is not required for correct folding of the enzyme but contributes to enzyme stability (Fig. 1A) (Xu *et al.*, 2011). We found that SptAH was incapable of folding correctly and maturation in the absence of a reducing agent (data not shown), most likely due to the presence of incorrectly paired disulfide bonds in the recombinant protein produced in *E. coli*. Therefore, the reducing agent DTT (10 mM) was added into the denaturation buffer to disrupt any incorrectly paired disulfide bonds in recombinant SptAH, and the denatured SptAH sample was diluted 10-fold to allow refolding and maturation of the enzyme in the presence of 1 mM DTT. Thus, it is not unexpected that some correctly folded SptAH molecules were converted into mature enzyme (M) molecules and then into $M^{\Delta C}$ and C″ before the formation of the Cys^{303}-Cys^{338} disulfide bond during the incubation.

The appearance of product C′, with an N-terminal sequence identified as ANEQ (Fig. 2F), was accompanied by the disappearance of SptAH (2–6 h, Fig. 2A), suggesting that C′ is the cleaved C-terminal portion of the precursor and that the cleavage occurs at Ser^{271}-Ala^{272} in the catalytic domain (Fig. 1A and Fig. 2F). Subsequently, 16 N-terminal residues were cleaved from C′, yielding product C* (6–24 h, Fig. 2A), which comprises only the CTE domain (Fig. 1A and Fig. 2F). It seems that early

**Fig. 2.** Maturation of SptAH and its derivatives.

A–E. Denatured S/A, SptAH or ΔS (0.65 μM) was diluted 10-fold with buffer A containing 4 M NaCl (A, B) or 4 M KCl (D) and then incubated at 37°C. At the time intervals indicated, samples were withdrawn and subjected to SDS-PAGE analysis and azocaseinolytic activity assay. The gels were stained with Coomassie brilliant blue G-250. The positions on the gels of the precursor (P), the proform (P^{ΔS}), the intermediate (I^{WT}), the mature form (M), the CTE-cleaved form of M (M^{ΔC}), the cleaved preprosequence (SN*), the cleaved core domain of the N-terminal propeptide (N*) and the cleaved C-terminal fragments (C*, C′, and C″) are indicated (A, B and D). Relative activity was calculated with the highest measured activity defined as 100% (A, B and D). The highest activities detected in samples of SptAH (8 h) and ΔS (8 h), as well as those of ΔSN* + SN* (Fig. 3A, 48 h), and ΔC (Fig. 3C, 54 h) were compared, with that of SptAH defined as 100% (C). The azocaseinolytic activities of samples (SptAH) activated in the presence of either 4 M KCl or 4 M NaCl were also compared, and the relative activity was calculated with the highest activity defined as 100% (E). Values are expressed as the means and standard deviations (error bars) of three independent experiments (C, E).

F. The amino acid sequence of SptA precursor composed of the signal peptide (S), the core domain of the N-terminal propeptide (N*), the linker peptide, and the mature enzyme (M) is shown. Active-site residues are boxed. The first four identified residues of the protein bands of P, I^{WT}, M, M^{ΔC}, SN*, C* and C′ (indicated by arrowheads in Fig. 2A) are underlined. N-terminal residues previously determined for the proform and fragment C″ (Xu *et al.*, 2011) are also underlined. Numbers indicate the positions of the amino acid residues, starting from the N-terminus of the mature enzyme.

maturing active enzyme not only degrades SN* and the linker peptide to accelerate enzyme maturation but also attacks the catalytic domain of the precursor, leading to the generation of products C′ and C*. This conclusion is supported by the results showing that although the addition of proteinase K accelerated the maturation process, the yield of the active mature form of SptAH was lower than in the absence of proteinase K (Fig. S1). Among the processing and degradation products, only I^{WT} was detected by anti–His-tag immunoblot analysis (data not

shown), suggesting that the C-terminal His-tag had been cleaved from M, C*, C′, and C″ (Fig. 1A). Considering that *in vitro* processing of SptAH was carried out under reducing conditions, the possibility that some of the degradation products (e.g., M^{ΔC}, C″, C*, and C′) are generated due to non-physiological reduction of the Cys^{303}-Cys^{338} disulfide bond cannot be excluded.

The purified sample of the recombinant proform of SptA (ΔS) contained more degradation products than that of SptAH (Fig. 1B). Also, more degradation products were
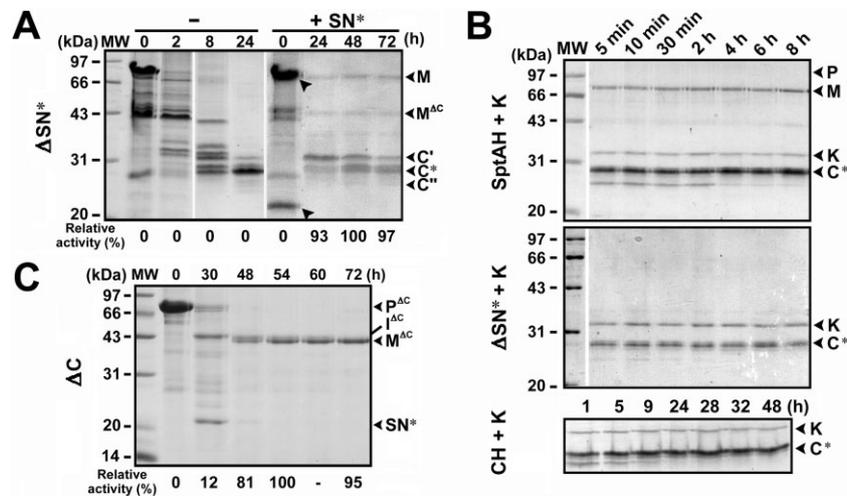
Fig. 3. Effects of the N-terminal propeptide and the CTE on folding and maturation of SptA.
A, C. Denatured ΔSN* (0.65 μM), either alone (−) or mixed with (+ SN*) an equal molar concentration of SN* (indicated by arrowheads) was diluted 10-fold with buffer A containing 4 M NaCl and incubated at 37°C (A). Denatured ΔC (0.65 μM) was also diluted 10-fold and incubated at 37°C (C). At the time intervals indicated, samples were withdrawn and subjected to SDS-PAGE analysis and azocaseinolytic activity assay. Relative activity was calculated with the highest measured activity defined as 100%.
B. Denatured SptAH, ΔSN*, or CH (0.65 μM) were diluted 10-fold with buffer A containing 4 M NaCl and incubated at 37°C. At the time intervals indicated, samples were withdrawn, incubated at 37°C with proteinase K (K, 0.05 μM) for another 1 h, and then subjected to SDS-PAGE analysis. The positions on the gels of the precursors (P and P$^{\Delta C}$), the intermediate (I$^{\Delta C}$), the wild-type mature form (M), the mature form derived from ΔC or the CTE-cleaved form of M (M$^{\Delta C}$), the cleaved preprosequence (SN*), and the cleaved C-terminal fragments (C*, C′, and C″) are indicated.

detected in the refolded ΔS sample than the SptAH refolded sample immediately after 10-fold dilution of the denatured samples (0 h, Fig. 2A and B). The reason for this phenomenon is presently unclear, probably because ΔS is less resistant to proteolysis by *E. coli* protease or active mature SptA than the precursor. As a result, the highest level of activity detected in the ΔS sample was lower than that in the SptAH sample (Fig. 2C). Nevertheless, ΔS showed a pattern of changes during the maturation process similar to that of SptAH (Fig. 2A and B). These results indicate that both the precursor and the proform of SptA mature via stepwise autoprocessing of the N-terminal propeptide and that the removal of the Tat signal peptide is not required for autocatalytic maturation of SptA.

Haloarchaea are known to accumulate molar concentrations of intracellular KCl to osmotically balance high external NaCl concentrations (Pérez-Fillol and Rodríguez-Valera, 1986; Martin *et al.*, 1999). The extracellular protease SptA is synthesized as a precursor within the cell and then secreted into the extracellular milieu in which it functions. We therefore investigated next whether SptAH can mature in the presence of KCl. As shown in Fig. 2D, denatured SptAH refolded and was converted into the active mature form in the presence of 4 M KCl; however, activation of SptAH was slower in 4 M KCl than 4 M NaCl (Fig. 2A and D). The highest level of activity exhibited by the enzyme activated in the presence of 4 M KCl was only ~ 30% of that of the enzyme activated in the presence of

4 M NaCl (Fig. 2E). These results suggest that autocatalytic maturation of SptA proceeds less efficiently in the presence of KCl than NaCl, and demonstrate a major difference in properties of SptA under conditions reflecting the intracellular (KCl) and extracellular (NaCl) environments respectively.

Effects of the N-terminal propeptide and CTE on folding and maturation of SptA

In contrast to SptAH and ΔS, which are converted to the mature form after refolding and processing, the variant ΔSN* (Fig. 1A) was degraded under the same conditions (Fig. 3A), suggesting that in the absence of the N-terminal propeptide, ΔSN* does not fold properly and adopts an unstable active conformation that undergoes autodegradation. Supporting evidence came from the finding that ΔSN* was more sensitive to proteinase K-mediated proteolysis than SptAH during refolding and maturation (Fig. 3B). When mixed with an equivalent molar amount of SN*, ΔSN* was converted into the active mature form after refolding and processing (Fig. 3A), although with a lower recovery of enzyme activity than that of SptAH (Fig. 2C). These results suggest that the N-terminal propeptide can act both *in cis* and *in trans* as a chaperone to facilitate the correct folding of SptA. In addition, during the maturation of SptAH and ΔS, complete release of enzyme activity was achieved only after the complete degradation of SN* or
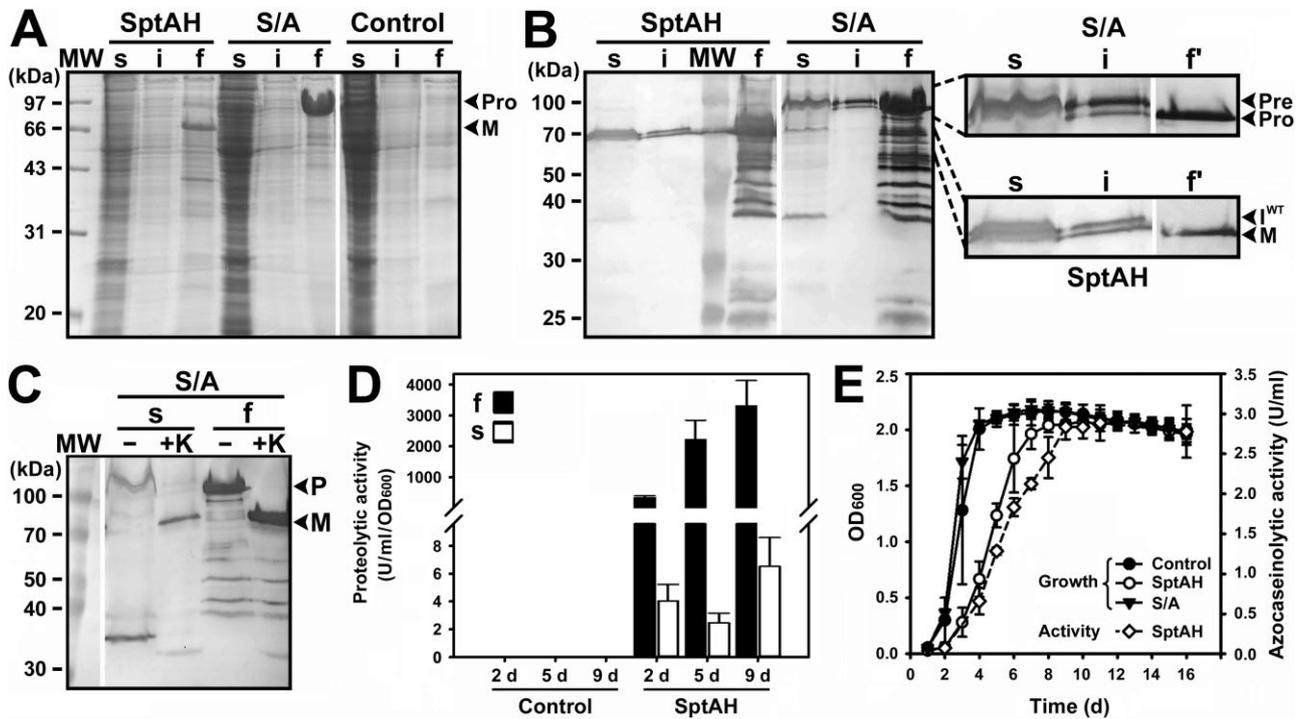
Fig. 4. Production and secretion of SptAH and S/A in *Hfx. volcanii*.

A, B. *Hfx. volcanii* harboring a blank vector (Control) or an expression vector for SptAH or S/A was grown in 18% MGM containing novobiocin (0.4 μg ml⁻¹) at 37°C. The culture supernatant (f), cell extract (s) and cell debris (i) from 0.5 ml of mid-log phase culture (OD_{600} = ~1.2) were subjected to SDS-PAGE (A) and anti–His-tag immunoblot analyses (B). Enlarged views of the bands of the precursor (Pre), the proform (Pro), the intermediate (I^{WT}), and the mature form (M) are visualized in the enlarged panels to the right, and the amount of culture supernatant loaded in lane f′ was one-twentieth of that in lane f (B).

C. The mid-log-phase culture supernatant (f) and cell extract (s) containing S/A were incubated at 37°C for 1 h in the absence (–) or presence (+ K) of proteinase K (0.15 μM) and then subjected to anti–His-tag immunoblot analysis. The positions on the gels of the (pre)proform (P) and the mature form (M) are indicated.

D. The proteolytic activities of the culture supernatant (f) and cell extract (s) of the culture of *Hfx. volcanii* harboring a blank vector (Control) or an expression vector for SptAH at different time points were measured using suc-AAPF-pNa as the substrate, and values are expressed as the means and standard deviations (error bars) of three independent experiments.

E. The growth of *Hfx. volcanii* harboring a blank vector (Control) or expression vector for SptAH or S/A was monitored by change in OD_{600}. The culture supernatants were subjected to azocaseinolytic activity assay. Values are expressed as the means and standard deviations (error bars) of three independent experiments.

N*, respectively (Fig. 2A and B), suggesting that the N-terminal propeptide also functions as an inhibitor of the mature form.

The CTE deletion variant ΔC (Fig. 1A) was converted into its mature form (M^{ΔC}) via stepwise autoprocessing of the N-terminal propeptide; however, the time required for full activation was much longer for ΔC (54 h, Fig. 3C) than SptAH or ΔS (8 h, Fig. 2A and B). Meanwhile, the highest level of activity detected in the ΔC sample was lower than those in the SptAH and ΔS samples (Fig. 2C). These results suggest that the CTE domain is not essential for folding but instead accelerates the folding and activation processes of the precursor or the proform of SptA. Proteinase K treatment of the refolding and processing samples of SptAH or ΔSN* led to the accumulation of product C*, which contains the CTE domain (Fig. 3B). Furthermore, when refolded alone, recombinant CTE (CH, Fig. 1A) was also resistant to proteolysis by proteinase K (Fig. 3B).

These results indicate that the CTE domain folds independently into a stable and proteolysis-resistant conformation. We previously found that the CTE domain stabilizes the catalytic domain (Xu *et al.*, 2011). It appears that the interaction between the CTE and catalytic domains is also beneficial for the folding and activation of SptA.

SptA is not only secreted from Hfx. volcanii *in a properly folded state but is also activated within and affects the growth of host cells*

To investigate whether the SptA precursor is activated within haloarchaeal cells, *Hfx. volcanii* was used as the host to produce SptAH and its active-site variant S/A. SDS-PAGE and Anti-His-tag immunoblot analyses of mid-log-phase culture samples showed that SptAH and S/A were predominantly localized in the culture supernatant in the mature form and proform, respectively (Fig. 4A and B),

indicating that *in vivo* maturation of SptA proceeds auto-catalytically. Evidence demonstrating that S/A exists in the precursor form in the cell extract and the proform in the culture supernatant (lanes s and f′, Fig. 4B) suggests that the signal peptide is cleaved by a host signal peptidase after secretion. After proteinase K treatment, both the intracellular S/A precursor and the extracellular S/A proform were converted into products with the same molecular weight as the mature form (75 kDa) (Fig. 4C), suggesting that both the precursor and proform of S/A are in the folded state and their conversion to 75-kDa products results from cleavage of their N-terminal propeptides by proteinase K. Notably, minor intermediate (I^{WT}) and mature (M) forms were detected in the cell extract of *Hfx. volcanii* producing SptAH (lane s, Fig. 4B). Using suc-AAPF-pNa as the substrate, proteolytic activity was detected in the cell extract of the strain producing SptAH but not in that of control strain harboring a blank vector (Fig. 4D) or the strain producing S/A (data not shown), indicating that the intracellular mature form of SptAH is active. Moreover, *Hfx. volcanii* cells producing SptAH grew slower than S/A-producing cells or control cells harboring a blank vector (Fig. 4E), suggesting that intracellularly activated mature SptA has a negative effect on the growth of host cells.

The minor precursor and proforms of S/A, I^{WT}, and the mature form of SptAH were detected in the cell debris (Fig. 4B), probably representing aggregates of denatured forms or those associated with cell debris. In addition, several degradation products of SptAH and the active-site variant S/A were detected in the cell extract and culture supernatant (Fig. 4B), indicating that the recombinant proteins underwent autodegradation (SptAH) and proteolysis by the host proteolytic system before and after secretion.

We next investigated whether mis/unfolded SptA is secreted via the Tat pathway. Based on the finding that the N-terminal propeptide is necessary for proper folding of SptA (Fig. 3A), the N-terminal propeptide deletion variant ΔN (Fig. 5) was constructed and produced in *Hfx. volcanii*. The variant ΔN was hardly detected by SDS-PAGE analysis, but most of the recombinant proteins in the cell extract could be detected as degradation products by anti-His-tag immunoblot analysis (Fig. 5). As the His-tag was fused at the C-terminus of ΔN and the molecular weight of the major degradation product was similar to that of the CTE domain (Fig. 5), cleavage of ΔN was determined to have occurred at the catalytic domain, suggesting that secretion of mis/unfolded ΔN via the Tat pathway is defective and that this protein, particularly its catalytic domain, is susceptible to degradation by the host proteolytic system. Conversely, the variant ΔNCD (which is comprised of only the signal peptide and the CTE domain) was detected in the culture supernatant by either SDS-PAGE or anti–His-tag immunoblot analysis (Fig. 5). As mentioned above, the CTE
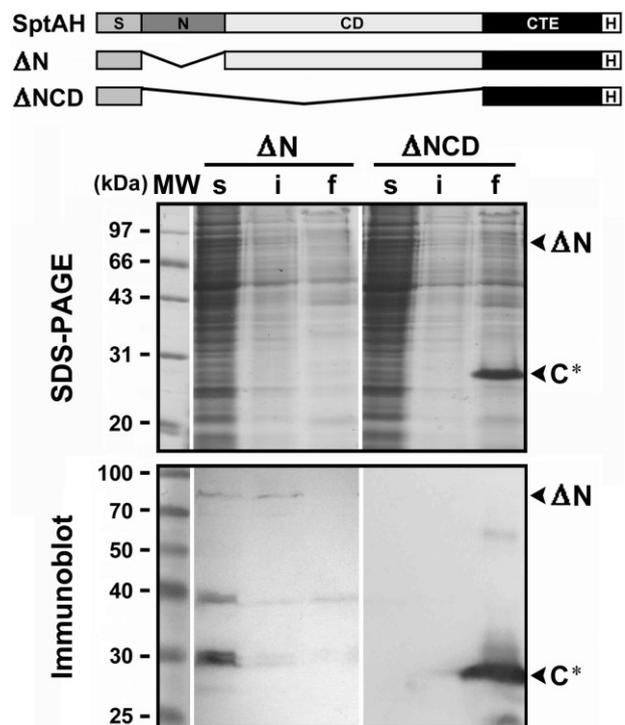

Fig. 5. Production and secretion of ΔN and ΔNCD in *Hfx. volcanii*. *Hfx. volcanii* harboring an expression vector for either ΔN or ΔNCD was grown to mid-log phase (OD_{600} = ~1.2) in 18% MGM containing novobiocin (0.4 μg ml⁻¹) at 37°C. The culture supernatant (f), cell extract (s) and cell debris (i) from 0.5 ml of the culture were subjected to SDS-PAGE and anti-His-tag immunoblot analyses. The positions on the gels of ΔN and the secreted form (C*) of ΔNCD are indicated. Schematic representations of SptAH, ΔN, and ΔNCD are shown at top.

domain folds independently into a stable, proteolysis-resistant conformation. In this context, *Hfx. volcanii* appears to possess a quality control system that degrades improperly folded proteins even if they have a Tat signal peptide but allows properly folded Tat substrates to be efficiently secreted.

Retarding the secretion of SptA in Hfx. volcanii *leads to intracellular accumulation of active mature enzyme and subsequent cell death*

Our previous study showed that substituting KK for the RR motif in the SptA signal peptide retards secretion of the enzyme in *Hfx. volcanii* (Shi *et al.*, 2006). In this study, we investigated the effect of retarding the secretion of SptA on the growth of *Hfx. volcanii*. A *Hfx. volcanii* strain harboring an expression plasmid for the RR motif variant (RR/KK) grew as red colonies on an 18% modified growth medium (MGM) agar plate after 12 days, but the colonies became pale after 24 days (Fig. 6A). In contrast, a *Hfx. volcanii* strain producing either SptAH or the active-site variant of RR/KK (RR/KK-S/A) grew as red colonies
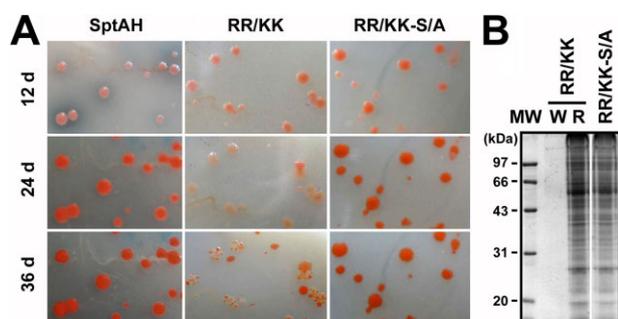
Fig. 6. Morphology of *Hfx. volcanii* colonies harboring an expression vector for SptAH, RR/KK or RR/KK-S/A. Each strain was grown on 18% MGM agar plates containing 1% skim milk and novobiocin (0.4 μg ml⁻¹) at 37°C, and colony morphology was recorded photographically (A). Cells of red (R) and pale (W) colonies of the strain harboring an expression vector for RR/KK and cells of colonies of the strain harboring an expression vector for RR/KK-S/A were scraped from the plates and subjected to SDS-PAGE analysis (B).

throughout the cultivation period under the same conditions (Fig. 6A), suggesting that RR/KK-derived activity was responsible for the fading colony color. The membrane of *Hfx. volcanii* is known to contain a high level of red-colored carotenoids, including lycopene. The fading colony color we observed was thus most likely due to destruction of the cellular metabolic machinery and cell lysis mediated by activated RR/KK. SDS-PAGE analysis revealed that the pale colony total cellular protein (TCP) sample contained only minor protein bands; however, the TCP sample of the red colony formed by *Hfx. volcanii* producing RR/KK-S/A contained considerably more proteins (Fig. 6B), indicating that RR/KK-derived activity is indeed involved in proteolysis of cellular proteins. Furthermore, subculturing of the pale colonies on an 18% MGM agar plate gave rise to far fewer colonies than did subculturing of the red colonies (data not shown), suggesting that most of the cells in the pale colonies were dead. It was noticed that a few small red colonies appeared on the pale colonies and on the plate after 36 days of growth of *Hfx. volcanii* harboring an expression plasmid for RR/KK (Fig. 6A). TCP of the small red colony showed similar protein pattern to that of the red colony formed by *Hfx. volcanii* producing RR/KK-S/A, rather than that of the pale colony (Fig. 6B). DNA sequencing of plasmids prepared from four small red colonies revealed that the RR/KK gene in these plasmids had undergone deletion/insertion-induced frameshift mutation (Fig. S2). Therefore, the emergence of the small red colonies is caused by a loss of RR/KK-derived activity in some cells during long-term cultivation, allowing the survival and multiplication of the host cells at later stage. Taken together, these results suggest that RR/KK-derived activity mediates the degradation of cellular proteins and cell death.

Next, we investigated the relationship between production of the recombinant proteins and host growth in liquid 18% MGM. The growth curve of the strain producing RR/KK-S/A was similar to that of the control strain harboring a blank vector (Fig. 7A). Anti–His-tag immunoblot analysis showed that RR/KK-S/A accumulated predominantly in the cell extract and the cell debris on day 3 in mid-log phase, and many degradation products of this protein were also detected (Fig. 7B). As the culture entered stationary phase (days 5 and 10), the amount of RR/KK-S/A in the cellular fraction decreased significantly (Fig. 7B), most likely due to degradation of the recombinant protein by the host proteolytic system. A relatively minor amount of RR/KK-S/A was detected in the culture supernatant even in the early (day 2) and mid (day 3) log phases (Fig. 7B), suggesting that secretion of RR/KK-S/A by *Hfx. volcanii* was retarded but not completely blocked.

Interestingly, the strain producing RR/KK exhibited a short initial log phase, followed by a long lag phase and a second log phase (Fig. 7A). This result was consistent with the observed emergence of small red colonies on the pale colonies after long-term (36 days) cultivation of the same strain on an 18% MGM agar plate (Fig. 6A). The biphasic growth pattern of this strain was not due to loss of novobiocin activity during the cultivation period, because supplementing the culture medium with novobiocin at the end of the long lag phase did not prevent the appearance of the second log phase (data not shown). The second log phase cells were grown on an 18% MGM agar plate, and plasmids from four single colonies were prepared for DNA sequencing. The results showed that these plasmids had undergone mutation, affecting RR/KK gene itself (Fig. S2). The mature form of RR/KK accumulated in the cell extract during the long lag phase (day 5, Fig. 7B). As the culture entered the second log phase (days 12 and 16), the amount of intracellular mature form decreased (Fig. 7B). This result was consistent with the observation that the intracellular proteolytic activity against suc-AAPF-pNa reached its highest level during the long lag phase but decreased during the second log phase (Fig. 7C). Conversely, using the same substrate, no proteolytic activity was detected in the cell extract of the strains producing RR/KK-S/A (data not shown) or harboring a blank vector (Fig. 4D). These results suggest that the biphasic growth pattern of the strain producing RR/KK is related to the level of active mature enzyme within the cell.

Sec-type signal peptide mediates secretion of SptA in Hfx. volcanii, but the secreted form undergoes proteolysis

To investigate whether the Sec-type signal peptide targets SptA for secretion via the Sec pathway, the Tat signal peptide of SptAH or S/A was replaced with the Sec signal
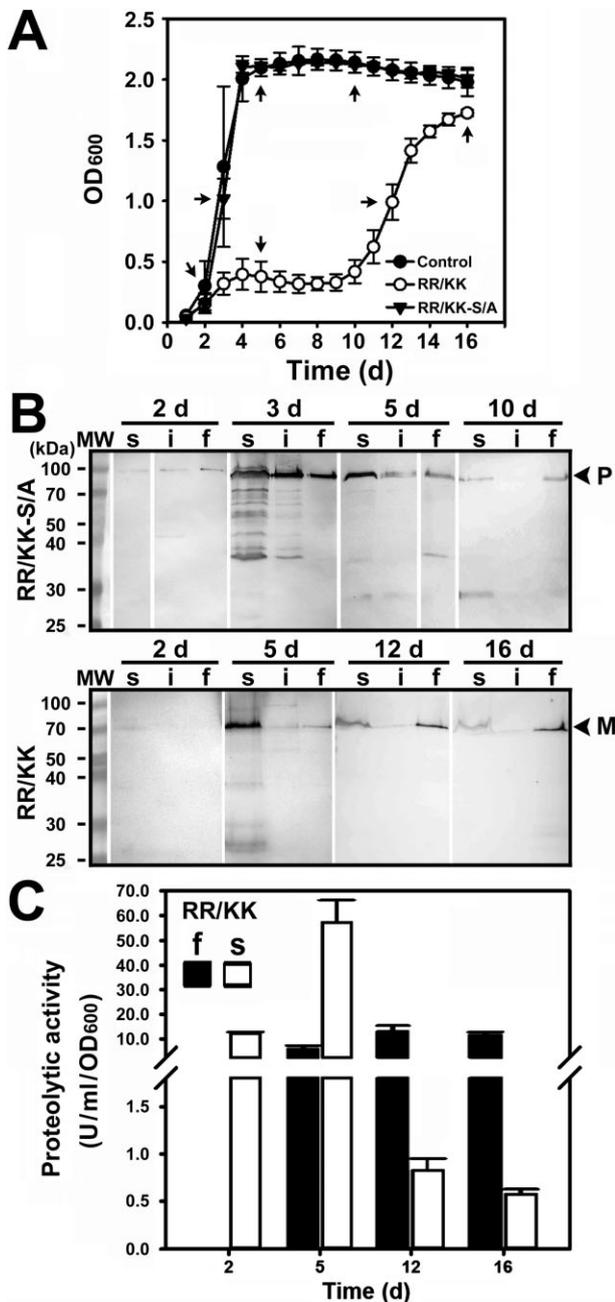
Fig. 7. Production and secretion of RR/KK and RR/KK-S/A in *Hfx. volcanii.*

Hfx. volcanii harboring a blank vector (Control) or an expression vector for RR/KK or RR/KK-S/A was grown in 18% MGM containing novobiocin (0.4 μg ml⁻¹) at 37°C. Growth was monitored by change in OD_{600} (A). At different time points as indicated by arrows (A), the culture supernatant (f), cell extract (s) and cell debris (i) from 0.5 ml of the culture were subjected to anti–His-tag immunoblot analysis (B) and proteolytic activity assay using suc-AAPF-pNa as the substrate (C). Values are expressed as the means and standard deviations (error bars) of three independent experiments (A, C). The positions on the gels of the (pre)proform (P) and the mature form (M) are indicated (B).

peptide of SptE, which is a subtilisin-like serine protease (NJ7G_0613) produced by *Natrinema* sp. J7-2 that has been detected in culture supernatant of this strain by proteomic analysis (Feng *et al.*, 2014). The resulting variants, designated Sec-SptAH and Sec-S/A, were produced in *Hfx. volcanii*. In both cases, no (pre)proform or mature form of either Sec-SptAH or Sec-S/A was detected, either intracellularly or extracellularly; however, a 40-kDa degradation product of the recombinant proteins was present in the culture supernatant (Fig. 8). This result suggests that the SptE Sec signal peptide mediates secretion of SptA into the medium, where it then undergoes proteolysis.

Sec-SptAH was also produced in *E. coli*, and the denatured recombinant protein was purified and subjected to *in vitro* refolding and processing. Sec-SptAH exhibited a maturation process similar to that of SptAH and ΔS (Figs 2A,B and 8B), indicating that proper folding and autocatalytic maturation of SptA is independent of either
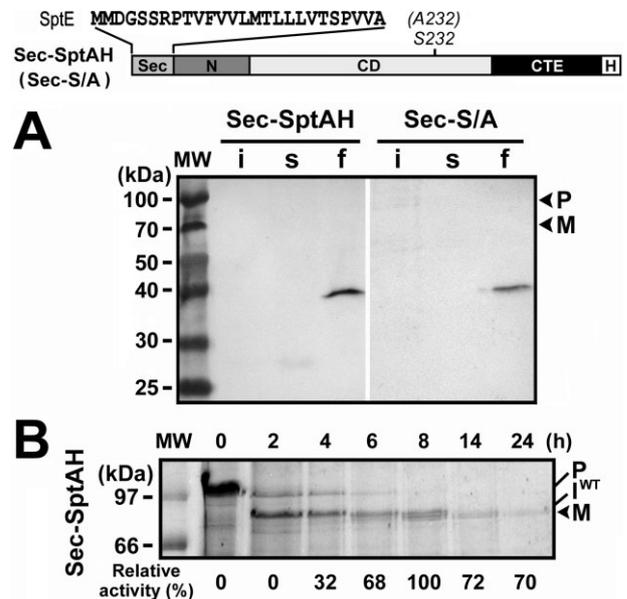
Fig. 8. Production and secretion of Sec-SptAH and Sec-S/A in *Hfx. volcanii.*

A. *Hfx. volcanii* harboring an expression vector either for the Sec-SptAH or Sec-S/A was grown to mid-log phase ($OD_{600} = \sim 1.2$) in 18% MGM containing novobiocin (0.4 μg ml⁻¹) at 37°C. The culture supernatant (f), cell extract (s) and cell debris (i) from 0.5 ml of the culture were subjected to anti–His-tag immunoblot analysis. The positions on the gels of the (pre)proform (P) and the mature form (M) are indicated. Schematic representations of Sec-SptAH and Sec-S/A are shown at top. The amino acid sequence of the Sec signal peptide of SptE (GenBank accession number AFO55867) is also shown.

B. Denatured Sec-SptAH (0.65 μM) was diluted 10-fold with buffer A containing 4 M NaCl and then incubated at 37°C. At the time intervals indicated, samples were withdrawn and subjected to SDS-PAGE analysis and azocaseinolytic activity assay. Relative activity was calculated with the highest activity defined as 100%. The positions on the gels of the precursor (P), the intermediate (Iᵂᵀ), and the mature form (M) are indicated.

the type or the presence of a signal peptide. Therefore, it is unlikely that degradation of the secreted form of Sec-SptAH in *Hfx. volcanii* is due to an intrinsic folding defect in the variant. Alternatively, the Sec substrates Sec-SptAH and Sec-S/A may be secreted in the unfolded state and thus susceptible to attack by the host proteolytic system until properly folded.

SptA is produced and secreted by Natrinema sp. J7-2 primarily during the stationary phase, and intracellular accumulation of the active mature form occurs during the stationary and death phases

The production, secretion, and maturation of SptA in *Natrinema* sp. J7-2 were also investigated. Strain J7-2 grew slightly better in 23% MGM than 18% MGM but exhibited a much higher level of extracellular azocaseinolytic activity when grown in 23% MGM (Fig. 9A), suggesting that the extracellular salt concentration plays an important role in the production of SptA. Minimal extracellular azocaseinolytic activity was detected during the early- and mid-log phases; however, this activity increased significantly in the late-log phase, reaching its highest level during the stationary phase (Fig. 9A). Consistent with this observation, immunoblot analysis revealed that the mature form of SptA accumulated primarily in the late-log-phase (4 days) and stationary-phase (10 days) culture supernatants (Fig. 9B). The minor proform, intermediate form, and mature form were detected in the culture supernatant on day 3 (Fig. 9B), suggesting that the *in vivo* maturation of SptA also occurs by stepwise processing of the N-terminal propeptide. The minor mature form of SptA was detected in the cell extract of stationary-phase cells grown in 23% MGM (10 days), and the amount of the intracellular mature form increased as the cells entered death phase (16 days) (Fig. 9B). In agreement with this observation, an increase in the level of intracellular proteolytic activity was detected during the transition from stationary to death phase (days 10 to 16) (Fig. 9C).

Discussion

Autocatalytic maturation of halolysin SptA

Both the *in vitro* and *in vivo* data presented here demonstrate that the maturation of SptA proceeds via stepwise autoprocessing of its N-terminal propeptide, which consists of a core domain (N*) and a 17-residue linker peptide. First, autocleavage of N* generates the intermediate I^WT, and then the linker peptide in I^WT is truncated in parallel with degradation of cleaved N*, yielding the active mature form composed of the subtilisin-like catalytic domain and the CTE domain (Fig. 10). Such a stepwise maturation process has been described for other linker peptide–
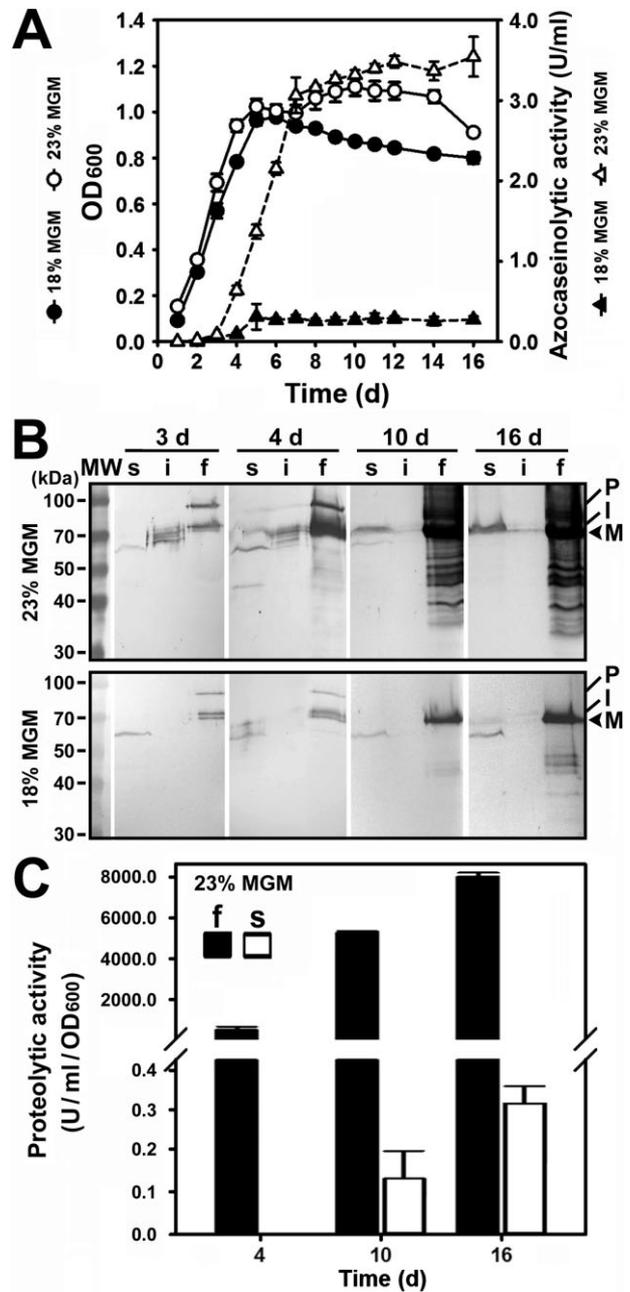
Fig. 9. Production and secretion of SptA in *Natrinema* sp. J7-2. Strain J7-2 was grown in 18 or 23% MGM at 37°C. Growth was monitored by change in OD_{600}, and the culture supernatants were subjected to azocaseinolytic activity assay (A). At the time intervals indicated, the culture supernatant (f), cell extract (s) and cell debris (i) from 0.5 ml of the culture were subjected to anti-SptA immunoblot analysis (B) and proteolytic activity assay using suc-AAPF-pNa as the substrate (C). Values are expressed as the means and standard deviations (error bars) of three independent experiments (A, C). The positions on the gels of the (pre)proform (P), the intermediate (I), and the mature form (M) are indicated (B).
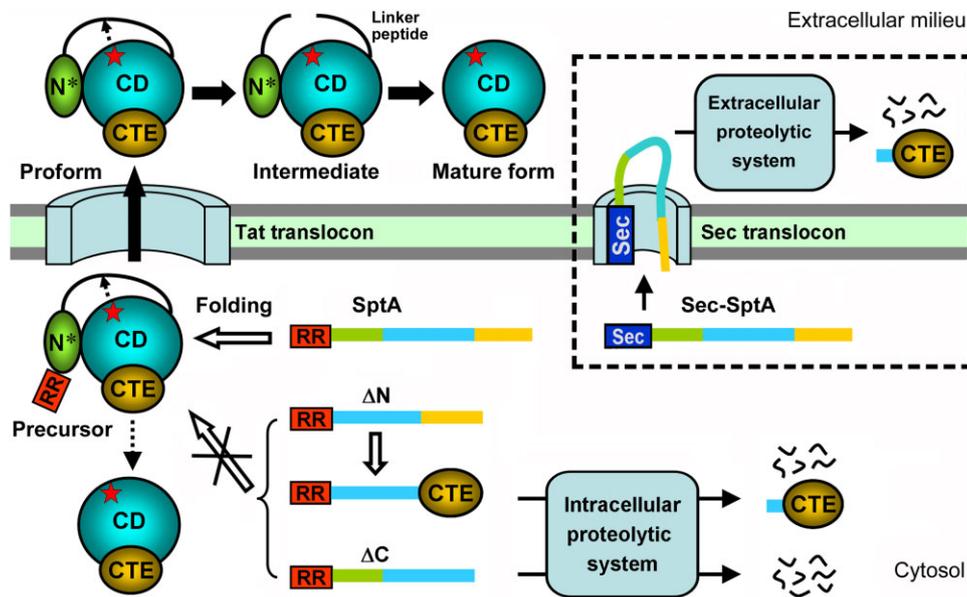
Fig. 10. Proposed model for secretion and activation of SptA.
After synthesis, the SptA precursor folds properly in the cytosol and is then targeted to the Tat translocon by its Tat signal peptide (RR). After secretion, the signal peptide is removed by a signal peptidase, releasing the proform into the extracellular milieu. Mediated by the active site (red star) of the catalytic domain (CD), the core domain (N*) of the N-terminal propeptide in the proform undergoes autocleavage to yield the intermediate. Next, the linker peptide is truncated and N* is degraded, generating the active mature form composed of the CD and the CTE domain. If not exported, the precursor matures autocatalytically in the cytosol (dashed arrow). The folding-defective variant ΔN is unable to be secreted via the Tat pathway but is degraded by the intracellular proteolytic system, leaving the CTE domain, which can fold independently into a proteolysis-resistant conformation. The variant ΔC folds too slowly and thus is sensitive to proteolysis. The variant Sec-SptA equipped with a Sec-type signal peptide (Sec) is secreted via the Sec pathway (in the dashed box). Sec-SptA is secreted in an unfolded state that is sensitive to proteolysis by the host extracellular proteolytic system. A proteolysis-resistant product comprised primarily of the CTE domain remains.

containing subtilases, including Tk-subtilisin (Tanaka *et al.*, 2007), protease CDF (Cheng *et al.*, 2009), WF146 protease (Zhu *et al.*, 2013), and SptC (Zhang *et al.*, 2014). For linker peptide-lacking subtilases such as subtilisins E (Yabuta *et al.*, 2001) and BPN′ (Gallagher *et al.*, 1995), following autocleavage of the N-terminal propeptide, the newly liberated N-terminus of the mature domain moves away from the active site and contributes to the formation of a Ca^{2+}-binding site (Yabuta *et al.*, 2002). Obviously, either truncation of the linker peptide or reorganization of the newly liberated mature domain N-terminus is beneficial for exposure of the active site and release of enzymatic activity.

It was recently reported that removal of the signal peptide may be necessary to facilitate the autocatalytic maturation of halolysin Nep from *Nab. magadii* (Ruiz *et al.*, 2012). Both the precursor and proform of SptA mature autocatalytically, indicating that removal of the signal peptide is not required for SptA activation. Therefore, it is not surprising that once folded properly, the SptA precursor is converted into its mature form intracellularly, providing it has not been exported.

Denatured SptA can be refolded and activated in the presence of high concentration of either NaCl or KCl, but the maturation efficiency of SptA in KCl solution is lower than in NaCl solution at equivalent salt concentrations. Our previous study demonstrated that SptA exhibits higher enzymatic activity in NaCl solution than KCl solution (Shi *et al.*, 2006). Because the maturation of SptA involves autocleavage and degradation of the N-terminal propeptide, the lower maturation efficiency in KCl solution is relevant to its lower activity in KCl. Although the preference of SptA for NaCl over KCl does not prevent intracellular SptA activity, it may contribute to a decreased toxicity of the enzyme prior to its export. A preference for NaCl over KCl has also been observed for other haloarchaeal enzymes, such as *Hfx. alicantei* β-galactosidase (Holmes *et al.*, 1997), *Hbt. salinarium* arginine deiminase (Monstadt and Holldorf, 1991), and *Natronococcus occultus* extracellular serine protease (Studdert *et al.*, 2001). Conversely, many other haloarchaeal enzymes show preference for KCl over NaCl (Lanyi, 1974; Ortega *et al.*, 2011). It appears that the salt preference depends on the nature of the enzyme, and thus a unified molecular mechanism remains elusive. Nevertheless, it has been reported that sodium binds at least twice as strongly to protein surfaces than potassium does, with the charged carboxylic groups of aspartate and glutamate playing the most important role (Vrbka *et al.*, 2006).

SptA possesses a high content of aspartate and glutamate residues (~ 18%), which are distributed primarily on the enzyme surface according to homology modelling (data not shown). In this context, it is reasonable to speculate that the higher affinity of the SptA surface for sodium over potassium may cause subtle structural changes in the enzyme in the presence of NaCl that are responsible for the difference in its enzymatic activity and maturation efficiency in the different salts.

Tat-dependent secretion of halolysin SptA

Tat substrates generally contain a consensus RR motif in their signal peptides. In contrast to RR-motif-containing wild-type SptA, which is efficiently secreted by *Hfx. volcanii* in a folded state, secretion of RR/KK or RR/KK-S/A is retarded, clearly indicating that SptA is a Tat substrate. However, substituting KK for the RR motif does not completely block secretion of the two variants. This is consistent with previous studies showing that KR, RK, and even KK motifs preserve the capacity of mediating Tat-dependent secretion of some bacterial proteins (Nivière *et al.*, 1992; Berks *et al.*, 2000; Stanley *et al.*, 2000; Buchanan *et al.*, 2001; DeLisa *et al.*, 2002; Ize *et al.*, 2002a,b). In addition, naturally occurring Tat signal sequences that lack one of the twin arginine residues have been reported for a few bacterial proteins (Hinsley *et al.*, 2001; Ignatova *et al.*, 2002; Widdick *et al.*, 2008). Therefore, in some signal peptide contexts, the consensus RR motif is not obligatory for Tat targeting, not only in bacteria but also in haloarchaea. Nevertheless, the secretion efficiency of RR/KK and RR/KK-S/A is markedly lower than that of wild-type SptA, demonstrating that the RR motif plays a key role in efficient secretion of the enzyme.

The decisive role for the signal peptide in targeting pathway specificity is reflected by the finding that SptA can be re-routed by a Sec signal peptide into the Sec pathway. Our results show that Sec-SptA and Sec-S/A are secreted into the culture medium by *Hfx. volcanii*; however, they undergo extracellular degradation by the host proteolytic system (Fig. 10). The secretion behaviors of the two artificial Sec substrates are distinctly different from that of SptAH, which is not only transported efficiently but also processed properly. In addition, the RR/KK variant is also nicely transported and correctly processed, although with a lower secretion efficiency than wild-type SptA. The distinct results with Sec-dependently transported Sec-SptA and Sec-S/A strongly support the Tat-dependence of secretion in case of the natural signal peptide of SptA. In *Hfx. volcanii*, roughly half of the ribosomes were found to bind to the membrane at the Sec translocon site and to mediate co-translational membrane protein insertion (Ring and Eichler, 2004). Post-translational secretion of fusion proteins with a Sec signal peptide has also been reported

in *Hfx. volcanii* (Irihimovitch and Eichler, 2003). Whether secretion of Sec-SptA or Sec-S/A occurs co- or post-translationally in *Hfx. volcanii* remains to be elucidated. If the two artificial Sec substrates are secreted post-translationally, they must be in an unfolded and translocation-competent state before secretion via the Sec pathway. In bacteria, cytoplasmic chaperones such as SecB bind precursors to prevent the formation of higher-order folded structures and then target them to SecA, a secretion-specific ATPase associated with the Sec translocon pore (Pohlschröder *et al.*, 2004). In contrast, very little is known about post-translational targeting and energetics in archaea. To date, a SecB homolog has been identified only in *Methanocaldococcus janaschii* (formerly *Methanococcus janaschii*) (Ha *et al.*, 2004), and SecA homologs are absent in archaea. Nevertheless, the existence of an archaeal protein structurally unrelated but functionally analogous to SecB or SecA cannot be excluded (Pohlschröder *et al.*, 2004). Notably, although denatured Sec-SptAH is capable of proper folding and autocatalytic activation *in vitro* in a manner similar to that of SptAH, no mature form of Sec-SptAH has been detected in the cellular fraction of *Hfx. volcanii*, in contrast to the case of SptAH, which can be converted into its mature form intracellularly. The presence of the Sec signal peptide in Sec-SptAH is the only feature that distinguishes it from SptAH with the Tat signal peptide. If post-translational secretion of Sec-SptAH or Sec-S/A occurs, the possible functional homolog of SecB in *Hfx. volcanii* would be expected to recognize the Sec signal peptide rather than the Tat signal peptide and to prevent proper folding of the enzyme *in vivo*. Investigation of this possibility awaits the identification and characterization of possible functional homologs of SecB and SecA in haloarchaea.

An appealing alternative explanation for the different secretion and activation behaviors of SptAH and Sec-SptAH in *Hfx. volcanii* is that whereas Tat-dependent secretion of SptAH occurs post-translationally, Sec-dependent secretion of Sec-SptAH occurs co-translationally and thus might not require a SecB-like chaperone and energy source. Confirmation of this possibility also awaits future experimental evidence, such as elucidation of the effect of the release of translocon-bound ribosomes on secretion of haloarchaeal Sec substrates. Regardless of the mechanism, whether co- or post-translationally, Sec-SptA and Sec-S/A are secreted in an unfolded state. Before being properly folded, the secreted forms of Sec-SptA and Sec-S/A are more sensitive to proteolysis by an as yet unidentified host extracellular proteolytic system than are SptAH and S/A, which are properly folded intracellularly and are proteolysis resistant (Fig. 10). Thus, from a biological standpoint, the Tat pathway is a better choice than the Sec pathway for secretion of SptA in haloarchaea.

The data presented here demonstrate that efficient secretion of SptA in haloarchaea depends not only on the presence of the Tat signal peptide but also on the folding state of the enzyme. For instance, the N-terminal propeptide is required for proper folding of SptA, and the N-terminal propeptide deletion variant ΔN, albeit equipped with a Tat signal peptide, is defective in secretion in *Hfx. volcanii*. In addition, *in vitro* analysis revealed that deletion of the CTE domain of SptA (ΔC) slows the folding rate of the enzyme, and our previous study demonstrated that the CTE-deletion variant SptAΔC125 (corresponding to ΔC) is also defective in transport across the cytoplasmic membrane of *Hfx. volcanii* (Xu *et al.*, 2011). In contrast, mediated by the Tat signal peptide, the CTE domain (which folds independently) is efficiently secreted into the culture medium by *Hfx. volcanii*. The mechanism by which the Tat pathway discriminates between folded and mis/unfolded substrates remains controversial. It has been proposed that the bacterial Tat translocon can intrinsically differentiate between folded and mis/unfolded substrates by a process termed 'folding quality control,' in which mis/unfolded proteins are recognized and rejected and their proteolysis initiated, resulting in export of only properly folded substrates (DeLisa *et al.*, 2003; Fisher *et al.*, 2006; Rocco *et al.*, 2012). Conversely, it has been suggested that no physiologically meaningful quality control takes place at the Tat translocon and that there is no need for an extra Tat-dependent degradation pathway, as the known cytoplasmic folding quality control systems (cytoplasmic chaperone and protease systems) adequately recognize and degrade mis/unfolded Tat substrates (Richter *et al.*, 2007; Lindenstrauß *et al.*, 2010). In both cases, however, because an exposed hydrophobic core is the typical hallmark of mis/unfolded proteins, the presence of hydrophobic surface patches on non-native Tat substrates is regarded as a determinant in blocking the secretion of such proteins via the Tat pathway through interaction of the patches with either membrane lipids (Richter *et al.*, 2007) or the Tat translocon (Rocco *et al.*, 2012). This rule appears to be applicable to Tat-incompatible SptA variants that are unable to fold properly (e.g., ΔN) or fold too slowly (ΔC). Evidence demonstrating the intracellular degradation of ΔN provides clear indication that mis/unfolded Tat substrates can be recognized by the *Hfx. volcanii* intracellular proteolytic system (Fig. 10), although it remains to be determined whether the degradation pathway is Tat-dependent or Tat-independent.

Relationship between intracellular activation of SptA and haloarchaeal growth

Owing to its capacity for autocatalytic maturation, the SptA precursor can be activated intracellularly if it has not been secreted into the culture medium. Our results demonstrate that intracellular activation of SptAH slows the growth of *Hfx. volcanii* and that intracellular accumulation of active mature enzyme is lethal to the haloarchaeon. Interestingly, RR/KK-producing *Hfx. volcanii* exhibits a biphasic growth curve composed of a short initial log phase, a long lag phase, and a second log phase. Such a growth pattern is related to the level of intracellular mature enzyme. Most likely, at the end of the initial log phase, the intracellular accumulation of active mature enzyme causes nonspecific proteolysis of cellular proteins and subsequent cell death. Thus, the cells enter a long lag phase in which they maintain a low level of growth. Evidence demonstrating that the RR/KK gene had undergone mutation in plasmids from the second log phase cells suggests that a loss or decrease of RR/KK-derived activity in some cells at the end of the long lag phase enables the culture to enter the second log phase.

In *Natrinema* sp. J7-2, production and secretion of SptA occurs during late log phase and peaks when the culture enters stationary phase. Similar observations have been reported for extracellular serine proteases of *Ncc. occultus* (Studdert *et al.*, 1997) and halolysin Nep of *Nab. magadii* (Giménez *et al.*, 2000). The extracellular protease of *Ncc. occultus* is induced by starvation and probably by a mechanism similar to quorum sensing (Paggi *et al.*, 2003). Nep is upregulated during the transition to the stationary phase in response to 'factors' (metabolites and/or regulatory molecules) present in high-density cultures of *Nab. magadii* (D'Alessandro *et al.*, 2007; Paggi *et al.*, 2010). In the case of SptA, its production level in *Natrinema* sp. J7-2 is highly dependent on the NaCl concentration in the culture medium, but its growth phase–dependent expression pattern is not influenced by a change in salt concentration, indicating that the production of SptA in its native host is strictly regulated by an as yet unknown mechanism. Obviously, production of SptA in the late-log and stationary phases can minimize the negative effect of intracellular activation of this enzyme on the cellular metabolic machinery, enabling *Natrinema* sp. J7-2 to reach a high population density by growing and dividing at the maximal rate during log phase. Moreover, the Tat pathway of strain J7-2 appears to be efficient enough for transport of SptA, thus reducing the possibility of intracellular activation of the enzyme. This hypothesis is supported by evidence showing that the ratio of intracellular to extracellular proteolytic activity in a stationary-phase strain J7-2 culture (10 days) (Fig. 9C) was only ~1:39 000, which is much lower than that of *Hfx. volcanii* producing SptAH (~1:500; Fig. 4D, 9 days). In this context, growth phase–dependent regulation of SptA synthesis in cooperation with a highly efficient secretion system appears to be crucial for preventing premature activation of this enzyme in *Natrinema* sp. J7-2. Additionally, *in vitro* analy-

sis revealed that autocatalytic maturation of SptA proceeds less efficiently in the presence of KCl than NaCl. Therefore, high intracellular KCl concentration in haloarchaea may also contribute to the suppression of premature activation of SptA, and limit detrimental effects on cells under normal growth conditions.

Studies of the physiologic role of halolysins are limited. It has been proposed that the accumulation of Nep in the extracellular medium at elevated cell densities enables more efficient scavenging of protein/peptide substrates in the natural environment by *Nab. magadii* (Paggi *et al.*, 2010). Likewise, SptA is produced and secreted by strain J7-2 primarily during the stationary phase, and thus may also serve a nutritional purpose by degrading external protein/peptide substrates at elevated cell densities. Additionally, the growth of strain J7-2 is slightly better in 23% MGM than 18% MGM, especially during the stationary phase, and the level of extracellular proteolytic activity is higher in 23% MGM. It is hypothesized that an increase in extracellular protease production may benefit the growth of strain J7-2 at higher salinity conditions by utilizing protein/peptide substrates more efficiently. However, it is clear that SptA does not play an essential role in the survival of *Natrinema* sp. J7-2, because strain J7-2 is capable of growth on synthetic media without amino acid supplements (Feng *et al.*, 2012). Moreover, it was observed that the amount of intracellular mature SptA increased as the J7-2 culture entered death phase, probably due to functional deterioration of the transport system in aged cells. Considering the lethal effect of intracellular mature SptA on *Hfx. volcanii*, the possibility that intracellular accumulation of mature SptA is involved in the transition of *Natrinema* sp. J7-2 culture from stationary to death phase cannot be excluded. From a physiologic viewpoint, the death of part of the population may provide nutrients for the surviving cells, thereby enhancing the survival of the haloarchaeal population as a whole.

In the present study, we showed that the Tat-dependent halolysin SptA matures autocatalytically and that premature activation of SptA in the heterologous host *Hfx. volcanii* affects its growth. However, in the native host, *Natrinema* sp. J7-2, the secretion and activation of SptA appear to be precisely regulated in order to prevent premature enzyme activation and proteolytic damage of cellular proteins during log-phase growth. We also found that intracellular accumulation of active SptA occurs during the stationary and death phases of strain J7-2. It would be interesting to determine if halolysins, a group of extracellular proteases involved in degradation of proteins and peptides in the natural environment, also participate in cell death and lysis to enhance survival of the haloarchaeal population in response to nutrient starvation.

Experimental procedures

Strains and growth conditions

Natrinema sp. J7 (CCTCC AB91141) was originally isolated from a salt mine in China (Shen and Chen, 1994). *Natrinema* sp. J7-2, a subculture of strain J7 lacking the plasmid pHH205 (Ye *et al.*, 2003; Feng *et al.*, 2012), was grown in MGM with 18% (18% MGM) or 23% (23% MGM) total salts, as described previously (Shi *et al.*, 2006). *Hfx. volcanii* WFD11 was used as the host for expression and was grown in 18% MGM supplemented with novobiocin (0.4 μg ml⁻¹) when necessary, as described previously (Shi *et al.*, 2006). *Escherichia coli* JM110 and *E. coli* BL21 (DE3) were used as cloning and expression hosts, respectively, and were grown at 37°C in Luria-Bertani (LB) medium supplemented with ampicillin (100 μg ml⁻¹) or kanamycin (30 μg ml⁻¹), as needed.

DNA manipulation, plasmid construction, and mutagenesis

Natrinema sp. J7-2 genomic DNA was prepared according to the method of Kamekura *et al.* (1992) and was used as the template for PCR. The primers used in this study are listed in Table S1. Plasmids pET26b (Novagen) and pTM11 (Chen, 2010) were used as vectors for expressing recombinant proteins in *E. coli* BL21 (DE3) and *Hfx. volcanii* WFD11 respectively. The pTM11 vector was derived from pTA230 (Allers *et al.*, 2004) by insertion of a *Sma*I-*Bam*HI fragment from pMLH32 encoding the novobiocin-resistance determinant (Holmes and Dyall-Smith, 2000) and a *Nsi*I-*Not*I PCR fragment encoding the hsp70 promoter from *Halobacterium salinarum* NRC-1 (Ng *et al.*, 2000). The genes encoding the wild-type SptA precursor (SptAH), the proform of SptA (ΔS), the preprosequence deletion variant (ΔSN*), the preprosequence (SN*), the CTE deletion variant (ΔC), and the CTE domain (CH) were amplified from genomic DNA by PCR using the primer pairs listed in Table S2. The N-terminal propeptide deletion variant (ΔN), the variant lacking the N-terminal propeptide and the catalytic domain (ΔNCD), and the signal peptide–replacement variant (Sec-SptAH) were constructed using the overlapping extension PCR method, as described previously (Bian *et al.*, 2006). Briefly, the 5′ and 3′ ends of target sequences were amplified from genomic DNA using the primer pairs listed in Table S2. The first-round 5′- and 3′-end PCR products were then used as templates in the second round of PCR without added primer. In the third round of PCR, intact genes encoding ΔN, ΔNCD, and Sec-SptAH were amplified using the primer pairs listed in Table S2. The above-mentioned amplified genes were then inserted into pET26b or pTM11 to generate expression plasmids for target proteins (Table S2). The QuikChange site-directed mutagenesis method (An *et al.*, 2010) was employed to construct the RR motif variant (KK) and the active-site variants of SptAH (S/A), KK (RR/KK-S/A), and Sec-SptAH (Sec-S/A) using the primers listed in Table S2. The sequences of all recombinant plasmids were confirmed by DNA sequencing.

Expression, in vitro *refolding, and activation*

Escherichia coli BL21 (DE3) cells harboring the pET26b-derived recombinant plasmids were grown at 37°C until the

optical density at 600 nm reached ~ 0.6. Production of recombinant proteins was induced by the addition of 0.4 mM isopropyl-β-D-thiogalactopyranoside and continued cultivation at 37°C for 4 h. The cells were then harvested and suspended in buffer A (50 mM Tris-HCl, 10 mM CaCl$_2$ [pH 8.0]) containing 8 M urea and disrupted by sonication on ice. After centrifugation at 13 000 × *g* for 10 min, the supernatant was collected and subjected to affinity chromatography on a column containing Ni^{2+}-charged chelating Sepharose Fast Flow resin (GE Healthcare) equilibrated with buffer A containing 8 M urea. After washing of the column with buffer A containing 8 M urea and 40 mM imidazole, bound proteins were eluted with buffer A containing 8 M urea and 100 mM imidazole. The purity of isolated proteins was assessed by SDS-PAGE. The concentration of purified samples was determined using the Bradford method (Bradford, 1976). The amount of target protein in the purified sample containing some degradation products was further assessed by band intensity measurement following SDS-PAGE, using bovine serum albumin as a standard.

To disrupt any incorrectly paired disulfide bonds in the recombinant proteins, samples containing purified protein were supplemented with 10 mM dithiothreitol (DTT) and kept at room temperature for 30 min. The samples of denatured protein were then diluted 10-fold with buffer A containing 4 M NaCl and incubated at 37°C to allow for protein refolding. During the incubation, aliquots of the samples were subjected to SDS-PAGE and azocaseinolytic activity assay.

Haloarchaeal growth and sample processing

The pTM11-derived plasmids for expressing SptAH and its derivatives were amplified in *E. coli* JM110 and then transferred into *Hfx. volcanii* WFD11 (Cline *et al.*, 1989). *Hfx. volcanii* WFD11 transformants were grown aerobically at 37°C with shaking at 180 rpm in 18% MGM containing 0.4 μg ml^{-1} of novobiocin. *Natrinema* sp. J7-2 was cultivated under the same conditions in 18 or 23% MGM. Haloarchaeal growth was monitored by measuring the culture optical density at 600 nm (OD$_{600}$).

Samples were withdrawn from cultures at various time points and cell-free culture supernatant was obtained by centrifuging the sample at 10 000 × *g* for 10 min at 4°C. The pelleted cells were washed 3 times with buffer A containing 3 M NaCl and sonicated on ice in the same solution. Subsequently, the supernatant (cell extract) and cell debris were separated by centrifugation at 13 400 × *g* for 10 min at 4°C. The cell debris was subjected to 3 successive washes with buffer A containing 3 M NaCl before use. The culture supernatant, the cell extract, and the cell debris were then used for immunoblot analysis and proteolytic activity assay.

Enzymatic activity assay

Azocaseinolytic activity was measured at 40°C for 60 min in 400 μl of reaction mixture containing 0.25% (w/v) azocasein (Sigma) and 200 μl of enzyme sample in buffer A containing 4 M NaCl. The reaction was terminated by adding 400 μl of 40% (w/v) trichloroacetic acid (TCA) to the reaction mixture. After incubation at room temperature for 15 min, the mixture was centrifuged at 13 400 × *g* for 10 min, and the absorbance of the supernatant at 366 nm (*A*$_{366}$) was measured in a 1-cm cell. One unit (U) of azocaseinolytic activity was defined as the amount of enzyme required to increase the *A*$_{366}$ by 0.01 per min under the assay conditions used.

Enzymatic activity against suc-AAPF-pNa (Sigma) was measured at 37°C in buffer A containing 3 M NaCl and 0.5 mM substrate. The initial velocity of suc-AAPF-pNa hydrolysis at 410 nm was monitored using a thermostat-controlled spectrophotometer (Cintra 10e, GBC, Australia), and the level of activity was calculated based on an extinction coefficient for *p*-nitroaniline (pNa) of 8480 M^{-1} cm^{-1} at 410 nm (DelMar *et al.*, 1979). One unit (U) of enzyme activity was defined as the amount of enzyme needed to produce 1 nmol of pNa per minute under the assay conditions.

SDS-PAGE and immunoblot analysis

Tris-glycine SDS-PAGE was carried out according to the method of King and Laemmli (1971). To prevent self-degradation of the protease during sample preparation (boiling), proteins were precipitated with TCA (final concentration of 20%), washed with acetone, solubilized in loading buffer containing 8 M urea, and then subjected to SDS-PAGE without prior heat treatment. After electrophoresis, proteins were transferred to a nitrocellulose membrane and subjected to immunoblot analysis using an anti-His-tag monoclonal antibody (Novagen) or anti-SptA polyclonal antibody (Xu *et al.*, 2011), as described previously (Cheng *et al.*, 2009).

N-terminal amino acid sequencing

After separation by SDS-PAGE, proteins were electroblotted onto a polyvinylidene difluoride membrane and stained with Coomassie Brilliant Blue R-250. Target protein bands were excised and subjected to N-terminal amino acid sequence analysis using a Procise 492 cLC peptide sequencer (Applied Biosystems).

References

Allers, T., Ngo, H.P., Mevarech, M., and Lloyd, R.G. (2004) Development of additional selectable markers for the halophilic archaeon *Haloferax volcanii* based on the *leuB* and *trpA* genes. *Appl Environ Microbiol* **70:** 943–953.

An, Y., Lv, A., and Wu, W. (2010) A QuikChange-like method to realize efficient blunt-ended DNA directional cloning

and site-directed mutagenesis simultaneously. *Biochem Biophys Res Commun* **397:** 136–139.

Berks, B.C., Sargent, F., and Palmer, T. (2000) The Tat protein export pathway. *Mol Microbiol* **35:** 260–274.

Berks, B.C., Palmer, T., and Sargent, F. (2005) Protein targeting by the bacterial twin-arginine translocation (Tat) pathway. *Curr Opin Microbiol* **8:** 174–181.

Bian, Y., Liang, X., Fang, N., Tang, X.F., Tang, B., Shen, P., and Peng, Z. (2006) The roles of surface loop insertions and disulfide bond in the stabilization of thermophilic WF146 protease. *FEBS Lett* **580:** 6007–6014.

Bolhuis, A. (2002) Protein transport in the halophilic archaeon *Halobacterium* sp. NRC-1: a major role for the twin-arginine translocation pathway? *Microbiology* **148:** 3335–3346.

Bradford, M.M. (1976) A rapid and sensitive method for the quantitation of microgram quantities of protein utilizing the principle of protein-dye binding. *Anal Biochem* **72:** 248–254.

Buchanan, G., Sargent, F., Berks, B.C., and Palmer, T. (2001) A genetic screen for suppressors of *Escherichia coli* Tat signal peptide mutations establishes a critical role for the second arginine within the twin-arginine motif. *Arch Microbiol* **177:** 107–112.

Chen, H. (2010) Primary analysis on the function of Hsp70 system from the archaeon *Haloferax volcanii*. Master degree thesis, Wuhan University, China.

Cheng, G., Zhao, P., Tang, X.F., and Tang, B. (2009) Identification and characterization of a novel spore-associated subtilase from *Thermoactinomyces* sp. CDF. *Microbiology* **155:** 3661–3672.

Cline, S.W., Lam, W.L., Charlebois, R.L., Schalkwyk, L.C., and Doolittle, W.F. (1989) Transformation methods for halophilic archaebacteria. *Can J Microbiol* **35:** 148–152.

D'Alessandro, C.P., De Castro, R.E., Giménez, M.I., and Paggi, R.A. (2007) Effect of nutritional conditions on extracellular protease production by the haloalkaliphilic archaeon *Natrialba magadii*. *Lett Appl Microbiol* **44:** 637–642.

De Castro, R.E., Maupin-Furlow, J.A., Gimenez, M.I., Seitz, M.K.H., and Sanchez, J.J. (2006) Haloarchaeal proteases and proteolytic systems. *FEMS Microbiol Rev* **30:** 17–35.

De Castro, R.E., Ruiz, D.M., Gimenez, M.I., Silveyra, M.X., Paggi, R.A., and Maupin-Furlow, J.A. (2008) Gene cloning and heterologous synthesis of a haloalkaliphilic extracellular protease of *Natrialba magadii* (Nep). *Extremophiles* **12:** 677–687.

DelMar, E.G., Largman, C., Brodrick, J.W., and Geokas, M.C. (1979) A sensitive new substrate for chymotrypsin. *Anal Biochem* **99:** 316–320.

DeLisa, M.P., Samuelson, P., Palmer, T., and Georgiou, G. (2002) Genetic analysis of the twin arginine translocator secretion pathway in bacteria. *J Biol Chem* **277:** 29825–29831.

DeLisa, M.P., Tullman, D., and Georgiou, G. (2003) Folding quality control in the export of proteins by the bacterial twin-arginine translocation pathway. *Proc Natl Acad Sci U S A* **100:** 6115–6120.

Dilks, K., Gimenez, M.I., and Pohlschröder, M. (2005) Genetic and biochemical analysis of the twin-arginine translocation pathway in halophilic archaea. *J Bacteriol* **187:** 8104–8113.

Feng, J., Liu, B., Zhang, Z., Ren, Y., Li, Y., Gan, F., *et al.* (2012) The Complete Genome Sequence of *Natrinema* sp. J7-2, a haloarchaeon capable of growth on synthetic media without amino acid supplements. *PLoS ONE* **7:** e41621.

Feng, J., Wang, J., Zhang, Y., Du, X., Xu, Z., Wu, Y., *et al.* (2014) Proteomic analysis of the secretome of haloarchaeon *Natrinema* sp. J7-2. *J Proteome Res* **13:** 1248–1258.

Fisher, A.C., Kim, W., and Delisa, M.P. (2006) Genetic selection for protein solubility enabled by the folding quality control feature of the twin-arginine translocation pathway. *Protein Sci* **15:** 449–458.

Gallagher, T., Gilliland, G., Wang, L., and Bryan, P. (1995) The prosegment-subtilisin BPN′ complex: crystal structure of a specific 'foldase'. *Structure* **3:** 907–914.

Giménez, M.I., Studdert, C.A., Sánchez, J.J., and De Castro, R.E. (2000) Extracellular protease of *Natrialba magadii*: purification and biochemical characterization. *Extremophiles* **4:** 181–188.

Grant, W.D. (2004) Life at low water activity. *Philos Trans R Soc Lond B Biol Sci* **359:** 1249–1267.

Ha, S.C., Lee, T.H., Cha, S.S., and Kim, K.K. (2004) Functional identification of the SecB homologue in *Methanococcus jannaschii* and direct interaction of SecB with trigger factor. *Biochem Biophys Res Commun* **315:** 1039–1044.

Hinsley, A.P., Stanley, N.R., Palmer, T., and Berks, B.C. (2001) A naturally occurring bacterial Tat signal peptide lacking one of the 'invariant' arginine residues of the consensus targeting motif. *FEBS Lett* **497:** 45–49.

Holmes, M.L., and Dyall-Smith, M.L. (2000) Sequence and expression of a halobacterial β-galactosidase gene. *Mol Microbiol* **36:** 114–122.

Holmes, M.L., Scopes, R.K., Moritz, R.L., Simpson, R.J., Englert, C., Pfeifer, F., and Dyall-Smith, M.L. (1997) Purification and analysis of an extremely halophilic β-galactosidase from *Haloferax alicantei*. *Biochim Biophys Acta* **1337:** 276–286.

Ignatova, Z., Hornle, C., Nurk, A., and Kasche, V. (2002) Unusual signal peptide directs penicillin amidase from *Escherichia coli* to the Tat translocation machinery. *Biochem Biophys Res Commun* **291:** 146–149.

Irihimovitch, V., and Eichler, J. (2003) Post-translational secretion of fusion proteins in the halophilic archaea *Haloferax volcanii*. *J Biol Chem* **278:** 12881–12887.

Ize, B., Gérard, F., Zhang, M., Chanal, A., Voulhoux, R., Palmer, T., *et al.* (2002a) *In vivo* dissection of the Tat translocation pathway in *Escherichia coli*. *J Mol Biol* **317:** 327–335.

Ize, B., Gérard, F., and Wu, L.F. (2002b) *In vivo* assessment of the Tat signal peptide specificity in *Escherichia coli*. *Arch Microbiol* **178:** 548–553.

Kamekura, M., Seno, Y., Holmes, M.L., and Dyall-Smith, M.L. (1992) Molecular cloning and sequencing of the gene for a halophilic alkaline serine protease (halolysin) from an unidentified halophilic archaea strain (172P1) and expression of the gene in *Haloferax volcanii*. *J Bacteriol* **174:** 736–742.

Kamekura, M., Seno, Y., and Dyall-Smith, M. (1996) Halolysin R4, a serine proteinase from the halophilic archaeon

Haloferax mediterranei; gene cloning, expression and structural studies. *Biochim Biophys Acta* **1294:** 159–167.

King, J., and Laemmli, U.K. (1971) Polypeptides of the tail fibres of bacteriophage T4. *J Mol Biol* **62:** 465–477.

Lanyi, J.K. (1974) Salt-dependent properties of proteins from extremely halophilic bacteria. *Bacteriol Rev* **38:** 272–290.

Lindenstrauß, U., Matos, C.F.R.O., Graubner, W., Robinson, C., and Brüser, T. (2010) Malfolded recombinant Tat substrates are Tat-independently degraded in *Escherichia coli*. *FEBS Lett* **584:** 3644–3648.

Madern, D., Ebel, C., and Zaccai, G. (2000) Halophilic adaptation of enzymes. *Extremophiles* **4:** 91–98.

Martin, D.D., Ciulla, R.A., and Roberts, M.F. (1999) Osmoadaptation in archaea. *Appl Environ Microbol* **65:** 1815–1825.

Monstadt, G.M., and Holldorf, A.W. (1991) Arginine deiminase from *Halobacterium salinarium*. Purification and properties. *Biochem J* **273:** 739–745.

Ng, W.V., Kennedy, S.P., Mahairas, G.G., Berquist, B., Pan, M., Shukla, H.D., *et al.* (2000) Genome sequence of *Halobacterium* species NRC-1. *Proc Natl Acad Sci USA* **97:** 12176–12181.

Nivière, V., Wong, S.L., and Voordouw, G. (1992) Site-directed mutagenesis of the hydrogenase signal peptide consensus box prevents export of a β-lactamase fusion protein. *J Gen Microbiol* **138:** 2173–2183.

Ortega, G., Lain, A., Tadeo, X., Lopez-Mendez, B., Castano, D., and Millet, O. (2011) Halophilic enzyme activation induced by salts. *Sci Rep* **1:** 6.

Paggi, R.A., Martone, C.B., Fuqua, C., and De Castro, R.E. (2003) Detection of quorum sensing signals in the haloalkaliphilic archaeon *Natronococcus occultus*. *FEMS Microbiol Lett* **221:** 49–52.

Paggi, R.A., Madrid, E.A., D'Alessandro, C.P., Cerletti, M., and De Castro, R.E. (2010) Growth phase-dependent biosynthesis of Nep, a halolysin-like protease secreted by the alkaliphilic haloarchaeon *Natrialba magadii*. *Lett Appl Microbiol* **51:** 36–41.

Pérez-Fillol, M., and Rodríguez-Valera, F. (1986) Potassium ion accumulation in cells of different halobacteria. *Microbiologia* **2:** 73–80.

Pohlschröder, M., Prinz, W.A., Hartmann, E., and Beckwith, J. (1997) Protein translocation in the three domains of life: variations on a theme. *Cell* **91:** 563–566.

Pohlschröder, M., Dilks, K., Hand, N.J., and Wesley Rose, R. (2004) Translocation of proteins across archaeal cytoplasmic membranes. *FEMS Microbiol Rev* **28:** 3–24.

Richter, S., Lindenstrauß, U., Lücke, C., Bayliss, R., and Brüser, T. (2007) Functional Tat transport of unstructured, small, hydrophilic proteins. *J Biol Chem* **282:** 33257–33264.

Ring, G., and Eichler, J. (2004) In the archaea *Haloferax volcanii*, membrane protein biogenesis and protein synthesis rates are affected by decreased ribosomal binding to the translocon. *J Biol Chem* **279:** 53160–53166.

Rocco, M.A., Waraho-Zhmayev, D., and DeLisa, M.P. (2012) Twin-arginine translocase mutations that suppress folding quality control and permit export of misfolded substrate proteins. *Proc Natl Acad Sci U S A* **109:** 13392–13397.

Rose, R.W., Brüser, T., Kissinger, J.C., and Pohlschröder, M. (2002) Adaptation of protein secretion to extremely high-salt conditions by extensive use of the twin-arginine translocation pathway. *Mol Microbiol* **45:** 943–950.

Ruiz, D.M., Paggi, R.A., Giménez, M.I., and De Castro, R.E. (2012) Autocatalytic maturation of the Tat-dependent halophilic subtilase Nep produced by the archaeon *Natrialba magadii*. *J Bacteriol* **194:** 3700–3707.

Shen, P., and Chen, Y. (1994) Plasmid from *Halobacterium halobium* and its restriction map. *Yi Chuan Xue Bao* **21:** 409–416.

Shi, W., Tang, X.F., Huang, Y., Gan, F., Tang, B., and Shen, P. (2006) An extracellular halophilic protease SptA from a halophilic archaeon *Natrinema* sp. J7: gene cloning, expression and characterization. *Extremophiles* **10:** 599–606.

Shinde, U., and Thomas, G. (2011) Insights from bacterial subtilases into the mechanisms of intramolecular chaperone-mediated activation of furin. *Methods Mol Biol* **768:** 59–106.

Siezen, R.J., and Leunissen, J.A.M. (1997) Subtilases: the superfamily of subtilisin-like serine proteases. *Protein Sci* **6:** 501–523.

Stanley, N.R., Palmer, T., and Berks, B.C. (2000) The twin arginine consensus motif of Tat signal peptides is involved in Sec-independent protein targeting in *Escherichia coli*. *J Biol Chem* **275:** 11591–11596.

Studdert, C.A., De Castro, R.E., Seitz, K.H., and Sanchez, J.J. (1997) Detection and preliminary characterization of extracellular proteolytic activities of the haloalkaliphilic archaeon *Natronococcus occultus*. *Arch Microbiol* **168:** 532–535.

Studdert, C.A., Herrera Seitz, M.K., Plasencia Gil, M.I., Sanchez, J.J., and De Castro, R.E. (2001) Purification and biochemical characterization of the haloalkaliphilic archaeon *Natronococcus occultus* extracellular serine protease. *J Basic Microb* **41:** 375–383.

Tanaka, S., Matsumura, H., Koga, Y., Takano, K., and Kanaya, S. (2007) Four new crystal structures of Tk-subtilisin in unautoprocessed, autoprocessed and mature forms: insight into structural changes during maturation. *J Mol Biol* **372:** 1055–1069.

Thomas, J.R., and Bolhuis, A. (2006) The tatC gene cluster is essential for viability in halophilic archaea. *FEMS Microbiol Lett* **256:** 44–49.

Vrbka, L., Vondrášek, J., Jagoda-Cwiklik, B., Vácha, R., and Jungwirth, P. (2006) Quantification and rationalization of the higher affinity of sodium over potassium to protein surfaces. *Proc Natl Acad Sci U S A* **103:** 15440–15444.

Widdick, D.A., Dilks, K., Chandra, G., Bottrill, A., Naldrett, M., Pohlschröder, M., and Palmer, T. (2006) The twin-arginine translocation pathway is a major route of protein export in *Streptomyces coelicolor*. *Proc Natl Acad Sci U S A* **103:** 17927–17932.

Widdick, D.A., Eijlander, R.T., van Dijl, J.M., Kuipers, O.P., and Palmer, T. (2008) A facile reporter system for the experimental identification of twin-arginine translocation (Tat) signal peptides from all kingdoms of life. *J Mol Biol* **375:** 595–603.

Xu, Z., Du, X., Li, T., Gan, F., Tang, B., and Tang, X.F. (2011) Functional insight into the C-terminal extension of halolysin SptA from haloarchaeon *Natrinema* sp. J7. *PLoS ONE* **6:** e23562.

Yabuta, Y., Takagi, H., Inouye, M., and Shinde, U. (2001) Folding pathway mediated by an intramolecular chaperone: propeptide release modulates activation precision of pro-subtilisin. *J Biol Chem* **276:** 44427–44434.

Yabuta, Y., Subbian, E., Takagi, H., Shinde, U., and Inouye, M. (2002) Folding pathway mediated by an intramolecular chaperone: dissecting conformational changes coincident with autoprocessing and the role of Ca^{2+} in subtilisin maturation. *J Biochem* **131:** 31–37.

Ye, X., Ou, J., Ni, L., Shi, W., and Shen, P. (2003) Characterization of a novel plasmid from extremely halophilic archaea: nucleotide sequence and function analysis. *FEMS Microbiol Lett* **221:** 53–57.

Zhang, Y., Wang, M., Du, X., Tang, W., Zhang, L., Li, M., *et al.* (2014) Chitin accelerates activation of a novel haloarchaeal serine protease that deproteinizes chitin-containing biomass. *Appl Environ Microb* **80:** 5698–5708.

Zhu, H., Xu, B.L., Liang, X., Yang, Y.R., Tang, X.F., and Tang, B. (2013) Molecular basis for auto- and hetero-catalytic maturation of a thermostable subtilase from thermophilic *Bacillus* sp. WF146. *J Biol Chem* **288:** 34826–34838.

Supporting information

Additional supporting information may be found in the online version of this article at the publisher's web-site.